American Mineralogist, Volume 91, pages 97–103, 2006

Phase transitions and volumetric properties of cryolite, Na_3AlF_6: Differential thermal analysis to 100 MPa

DAVID DOLEJŠ* AND DON R. BAKER

Department of Earth and Planetary Sciences, McGill University, 3450 rue University, Montreal, Quebec H3A 2A7, Canada

ABSTRACT

Cryolite, Na_3AlF_6, is the most abundant aluminofluoride mineral in highly evolved felsic suites and their pegmatites, but its phase transitions and thermodynamic properties at elevated pressures are unknown. We used a simple modification of the TZM pressure vessel to perform differential thermal analysis of cryolite at high pressures. Temperatures of the α-β transition are as follows: 559.30 ± 0.23 °C (1 atm), 562.10 ± 0.28 °C (47 MPa), and 567.33 ± 0.23 °C (101 MPa). Cryolite melting temperatures increase as follows: 1011.4 ± 0.2 °C (1 atm), 1019.2 ± 0.4 °C (50 MPa), and 1028.7 ± 0.4 °C (100 MPa). Both pressure-temperature relationships are linear: $(dT/dp)_{\alpha\text{-}\beta} = 78.4 \pm 8.4$ °C/GPa and $(dT/dp)_m = 174 \pm 12$ °C/GPa. Application of the Clapeyron relationship leads to the following volumetric changes: $\Delta V_{\alpha-\beta} = 0.089 \pm 0.019$ J/(mol·bar) and $\Delta V_m = 1.49 \pm 0.12$ J/(mol·bar). Despite the significant self-dissociation in the cryolite liquid, melting sensu stricto (without dissociation) dominates the heat and volumetric changes during melting in comparable amounts: 83.3 ± 6.7 % ΔH_m and 68 ± 15 % ΔV_m and suggests that the degree of dissociation has no significant effect on the $(dT/dp)_m$. Evaluation of previous and current volumetric data for cryolite polymorphs leads to $V_{\beta,1284} = 8.49 \pm 0.17$ J/(mol·bar); coefficients for the volumetric thermal expansion in the form of the third-order polynomial equation are: $V_{298} = 7.080 \pm 0.012$ J/(mol·bar), $a_1 = (1.39 \pm 0.20)\cdot10^{-4}$ K^{-1}, $a_2 = (-2.15 \pm 0.51)\cdot10^{-7}$ K^{-2}, and $a_3 = (2.68 \pm 0.34)\cdot10^{-10}$ K^{-3}. The total $(dT/dp)_m$ of cryolite is very similar to that of villiaumite (NaF), whereas $\Delta V_m/V_{\beta,1284}$ of cryolite is smaller than for other alkali halides (NaF, NaCl).

Keywords: DTA, TGA, cryolite, phase transition, thermodynamics

INTRODUCTION

Cryolite, Na_3AlF_6 (Abildgaard 1799), is the most abundant aluminofluoride mineral in nature (Bailey 1980). Cryolite occurs as two polymorphs: low-temperature monoclinic α-cryolite and high-temperature orthorhombic (pseudocubic) β-cryolite (Strunz and Nickel 2001; Yang et al. 1993), which are separated by a first-order displacive phase transition at ~563 °C and 1 atm (Spearing et al. 1994; Chase 1998). Na_3AlF_6 is a neso-aluminofluoride (Brosset 1937; Pabst 1950; Hawthorne 1984) containing corner-sharing octahedra $[AlF_6]$ and $[NaF_6]$ with additional sodium atoms in cubic and 12-fold coordination: α-$Na_2^{[8]}Na^{[6]}[AlF_6]$ and β-$Na_2^{[12]}Na^{[6]}[AlF_6]$ (Hawthorne and Ferguson 1975; Strunz and Nickel 2001). Cryolite forms two solid solutions: Na_3AlF_6-AlF_3 with the $AlNa_{-3}$ substitution (Dewing 1978, 1997) and Na_3AlF_6-$NaCaAlF_6$ with the $CaNa_{-2}$ exchange (Craig and Brown 1980; Lin et al. 1982). The melting point of β-cryolite is 1012 °C at 1 atm (Chase 1998) and cryolite melt is a highly conductive, ionic liquid (Landon and Ubbelohde 1956) with about 30–40% self-dissociation of octahedral AlF_6^{3-} ions into free F^-, tetrahedral AlF_4^-, and pentahedral AlF_5^{2-} ions (Feng and Kvande 1986; Xu et al. 2001).

Cryolite occurs in peralkaline granites and pegmatites (Goodenough et al. 2000) and $Na_4Al_{1.333}F_8$ is a component for quasicrystalline models of F-bearing melts (Burnham 1997). Interactions between cryolite and fully polymerized silicate melts reflect incorporation mechanisms of fluorine in the silicate framework and local avoidance principles (Dolejš and Baker 2004b) and lead to the occurrence of the fluoride-silicate liquid immiscibility (Kogarko 1967; Kogarko and Krigman 1975; Rutlin 1998). The liquid-liquid immiscibility propagates into the quartz-albite-cryolite-topaz quaternary system (Dolejš and Baker 2001, 2002), and must be evaluated as a petrogenetic phenomenon in the differentiation of F-bearing felsic magmas.

Due to its significance in electrolytic metallurgy (Grjotheim et al. 1977), the thermodynamics of Na_3AlF_6 is well known at ambient pressure (Chase 1998; Chartrand and Pelton 2002). However, the temperatures of the α-β transition and melting at high pressures as well as the associated volumetric changes are not available. In this study, we use differential thermal analysis in the TZM pressure vessel to determine temperatures of the cryolite phase transition and melting to 100 MPa. We report temperature measurements and derive volumetric changes of the α-β phase transition, melting, and partial dissociation of Na_3AlF_6 to 100 MPa. These data provide basis for phase-equilibria studies and thermodynamic models of cryolite-bearing granitic melts.

EXPERIMENTAL TECHNIQUE

Temperatures of the Na_3AlF_6 transition and melting were measured by differential thermal analysis in the TZM pressure vessel. The starting material was hand-picked crystalline cryolite (99.5%, Alfa Aesar). Microprobe analysis revealed 32.34 ± 0.15 wt% Na, 12.96 ± 0.35 wt% Al, 54.68 ± 0.49 wt% F, and <0.10 wt%

* Present address: Bayerisches Geoinstitut, Universität Bayreuth, D-95440 Bayreuth, Germany. E-mail: david.dolejs@uni-bayreuth.de

K, Ca, and Si (average of 10 measurements, standard deviations 1 σ), which corresponds to the formula $Na_{2.93(4)}Al_{1.00(3)}F_6$. The cryolite powder was stored permanently at 120 °C to prevent absorption of moisture. Platinum tubing was cleaned in concentrated hydrofluoric acid, repeatedly washed with distilled water, cleaned in the ultrasonic bath, and annealed to orange heat. After loading with cryolite powder, crimped capsules were stored at 300 °C for one hour to remove remaining traces of moisture (less than 0.2 wt%) and were welded shut immediately afterward. Two platinum capsules were used in the experiments: a flat-welded capsule with 66.92 mg cryolite for the 1 atm experiments and a re-entrant capsule with 55.34 mg cryolite for experiments at elevated pressures.

Preliminary 1 atm experiments were performed in a tube furnace (30.5 cm long, 4.1 cm inner diameter), which contained two parallel chromel-alumel thermocouples. The platinum capsule and one of the thermocouples were wrapped together with copper foil. The distance between the sample and the reference thermocouple was 8–10 mm in air.

Experiments at elevated pressures were carried out in a vertical TZM pressure vessel with argon gas as the pressure medium (Fig. 1). An internal, sheathed thermocouple leads through the high-pressure T-junction into the sample chamber and its tip is in the re-entrant capsule. An external sheathed thermocouple is inserted into the well in the inconel sheath (Fig. 1). Temperatures were scanned simultaneously in one or five second steps and converted via a PCI-DAS-TC hardware card (Computer Boards, Inc.) into a spreadsheet format. Instrumental fluctuation in the temperature log is ±0.06 °C. During all measurements, both thermocouples were ground to a common pole to eliminate false currents induced by the furnace winding.

Chromel-alumel thermocouples were calibrated against the melting points of pure salts at 1 atm: NaCl = 800.7 °C (Dawson et al. 1963; Chase 1998), Na_2SO_4 = 883.6 °C (Kleppa and Julsrud 1980), and NaF = 992.5 °C (Kojima et al. 1968; Kleppa and Julsrud 1980). The temperature calibration is accurate to 0.4 °C. Pressure was monitored with the Bourdon-tube pressure gauges and is accurate to 5 MPa.

RESULTS

The thermal effects of the phase transition and melting were evaluated by calculating the temperature difference between the internal (sample) and external (reference) thermocouples and normalizing to the background defined by the internal thermocouple outside of the thermal peaks. All transitions are bracketed by the opposite displacements observed in the heating and cooling curves, respectively. The terminology and geometry of thermal effects are illustrated in Figure 2.

The α-β solid-state transition is characterized by a symmetrical endothermic peak during heating and a symmetrical exothermic peak during cooling. In most experiments the onsets of the thermal effect are identical or overlap within the error bracket of the temperature measurements. In one case, the endothermic effect was delayed by 3.9 °C, probably due to the high heating rate in this experiment (7.8 °C/min). The measured temperatures of the α-β transition at 1 atm, 50 MPa, and 100 MPa are presented in Table 1. The increase in the transition temperature with pressure is linear and the least-squares fit, for variables with independent errors (Reed 1989, 1992), yields $(dT/dP)_{\alpha\text{-}\beta}$ = 78.4 ± 8.4 °C/GPa, i.e., 7.84 ± 0.84 °C/kbar (Fig. 3).

The melting and crystallization of cryolite show thermal effects related to melting initiation and the melting reaction, as well as crystallization delayed by undercooling. The initiation of melting is a slow onset of the endothermic reaction several degrees Celsius before the melting temperature is reached; this phenomenon is a common feature during differential thermal analysis (e.g., Wyllie and Raynor 1965; Koster van Groos 1979). The effect of the endothermic onset is very small (<5 °C, Table 1) and insignificant for melt production before reaching the congruent melting point. The onset of cryolite melting is manifested by an inflection prior to the endothermic maximum (Fig. 2c).

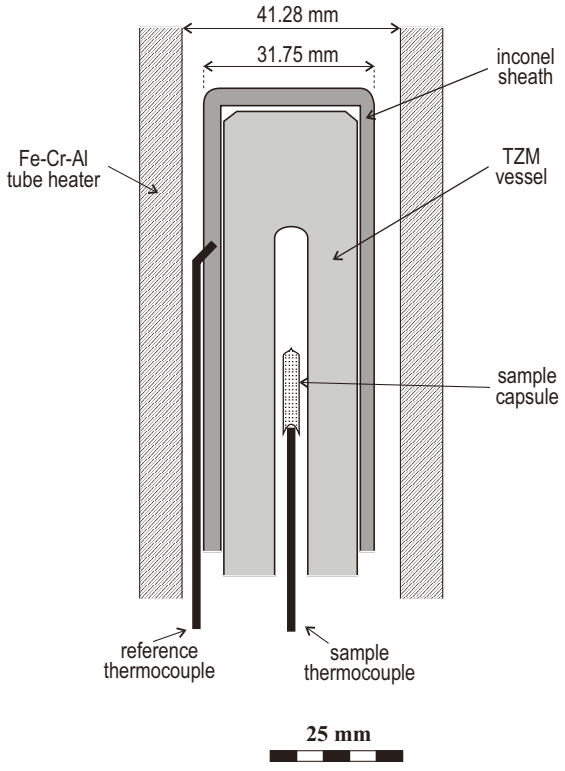

FIGURE 1. The TZM pressure vessel for differential thermal analysis with location of sample capsule and thermocouples.

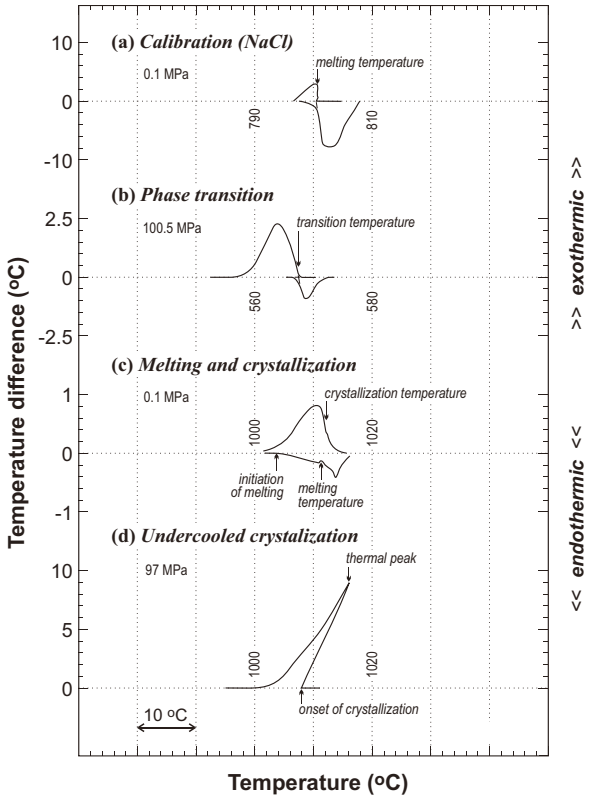

FIGURE 2. Geometry and terminology of thermal effects.

TABLE 1. Differential thermal analysis of the α-β cryolite phase transition

Pressure (MPa)	Thermal onset (°C)	Heating/cooling rate (°C/min)
0.1	559.0	2.47 (h)
	563.2*	7.84 (h)
	559.6	2.39 (c)
	559.3	4.01 (c)
	559.30 ± 0.23	average
47	562.2	2.69 (h)
	562.0	5.77 (c)
	562.10 ± 0.28	average
100.5	566.9	1.27 (h)
	567.8	2.47 (h)
	567.3	5.82 (c)
	567.33 ± 0.23	average

Notes: Individual temperature measurements are accurate to ±0.4 °C. Abbreviations: h = heating path, c = cooling path. Rates are measured immediately prior to the onset of the thermal event.
* Value not included in the average.

TABLE 2. Differential thermal analysis of the Na_3AlF_6 melting

Pressure (MPa)	Thermal events (°C)			Heating/cooling rate (°C/min)
0.1	1009.2 (im)	1011.9 (m)	1014.1 (p)	0.36 (h)
		1009.9 (m)	1014.7 (p)	1.05 (h)
		1011.3 (m)		2.82 (h)
		1012.3 (x)*	1011.2 (p)	0.89 (c)
	997.2 (x)	1002.0 (p)		0.53 (c)
	992.2 (x)	997.6 (p)		9.54 (c)
		1011.4 ± 0.2		melting
51.5	1014.8 (im)	1019.2 (m)	1020.3 (p)	3.28 (h)
	1008.0 (x)	1016.2 (p)		1.65 (c)
		1019.2 ± 0.4		melting
97	1016.0 (im)	1028.7 (m)	1030.9 (p)	3.27 (h)
	1025.5 (x)	1028.8 (p)		0.94 (c)
		1028.7 ± 0.4		melting

Notes: Individual temperature measurements are accurate to ±0.4 °C. Abbreviations: im = initiation of melting, m = melting, p = thermal peak, x = onset of crystallization; h = heating, c = cooling.
* Experiment reversed before melting was complete to preserve cryolite nuclei.

This point corresponds to the equilibrium liquidus temperature in other salt systems (Fig. 2a, cf. Koster van Groos 1979), and is interpreted as the melting temperature.

During cooling, many experiments display metastable undercooling due to the delayed nucleation of cryolite (cf. Yamada et al. 1993). We distinguish the onset of crystallization and the peak temperature (Fig. 2d); the peak temperature is higher than the onset of crystallization (by 3–8 °C, Table 2) due to the release of the latent heat of crystallization. Experiments with identical crystallization onset and temperature show overlap with the melting temperature on the heating curve, thus are indicative of the equilibrium liquidus temperature (Fig. 2a).

All these effects were observed due to the high resolution and recording frequency of our experimental procedure. The cryolite melting interval remains delimited by the endothermic and exothermic maxima during heating and cooling, respectively, and these bracket the melting points in all experiments (Table 1). All experimental measurements at ambient and elevated pressures are reported in Table 2. The melting temperature of cryolite increases linearly with pressure within the error brackets, and this allows us to calculate the pressure-temperature dependence: $(dT/dP)_m$ = 174 ± 12 °C/GPa, i.e., 17.4 ± 1.2 °C/kbar (Fig. 3).

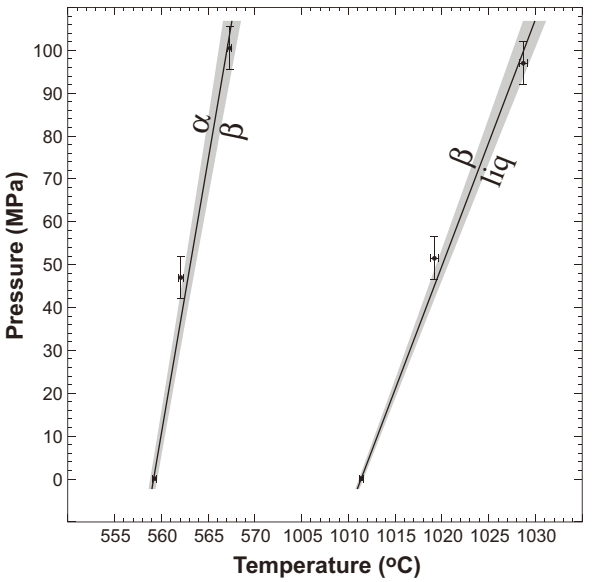

FIGURE 3. Pressure-temperature diagram for the α-β transition and melting of cryolite. Gray intervals are uncertainty limits of the fit at 1σ.

VOLUME CHANGES DURING PHASE TRANSITIONS

The linear pressure-temperature dependence of the α-β conversion and melting temperature for cryolite is utilized to calculate the volume changes of phase transitions. The differential of the Gibbs-Duhem relationship leads to the Clapeyron relationship (Prigogine and Defay 1954; Denbigh 1981; Stølen and Grande 2004):

$$\frac{dp}{dT} = \frac{\Delta H_{tr}}{T_{tr} \cdot \Delta V_{tr}} \quad (1)$$

with T_{tr}, ΔH_{tr}, and ΔV_{tr} are the temperature, enthalpy, and volume of the transition, respectively.

The enthalpy of the α-β transition has been estimated between 9.0 and 10.0 kJ/mol (O'Brien and Kelley 1957; Majumdar and Roy 1965) and we adopt a value of 9.5 ± 1.7 kJ/mol in accordance with Chase (1998). By using Equation 1 with $T_{\alpha\text{-}\beta}$ = 832.45 ± 0.23 K at 1 atm (Table 1), we obtain $\Delta V_{\alpha\text{-}\beta}$ = 0.089 ± 0.019 J/(mol·bar). The enthalpy of cryolite melting varies between 107 and 116 kJ (Malinovský 1984; Sterten and Mæland 1985); the value from Chase (1998), ΔH_m = 110.0 ± 5.0 kJ/mol, is representative of this range and maintains consistency with thermochemical compilation by Dolejš and Baker (2004a). The corresponding volume change during melting at T_m = 1284.55 ± 0.20 K (Table 2) is ΔV_m = 1.49 ± 0.12 J/(mol·bar).

THERMAL EXPANSION OF CRYOLITE

The present experimental results provide the molar volume of β-cryolite at its melting point from the melt density (Edwards et al. 1953; Fernandez and Østvold 1989) and the volume change of melting, ΔV_m. This datum complements previous X-ray diffraction measurements of the thermal expansion of cryolite to 900 K (Stewart and Rooksby 1953; Yang et al. 1993) and yields the thermal expansion parameters from room conditions to the melting temperature.

The molar volume of the cryolite melt at its melting point, 1011 °C, is $V_{liq,1284}$ = 9.98 ± 0.12 J/bar (Fernandez and Østvold 1989), which is equal to previous density measurements (Edwards et al. 1953). Subtraction of the volume change during

melting yields a molar volume for β-cryolite at 1011 °C, $V_{\beta,1284}$ = 8.49 ± 0.17 J/bar. This value lies on the extension of the non-linear thermal-expansion trend of cryolite (Fig. 4).

To describe the non-linear thermal behavior, we use the third-order polynomial expansion of molar volume in temperature:

$$V_T = V_{298} \cdot \left\{1 + a_1 \cdot (T - 298.15) + a_2 \cdot (T - 298.15)^2 + a_3 \cdot (T - 298.15)^3\right\} \quad (2)$$

where $V_{298.15}$ and V_T are molar volumes at reference state (298.15 K) and temperature of interest, respectively, and T is temperature (K). The thermal expansion coefficient (expansivity) for solids, α, has the following form:

$$\alpha = \frac{1}{V} \cdot \left(\frac{\partial V}{\partial T}\right) \quad (3)$$

Values of regression coefficients, a_i, were obtained by linear least-square fitting of the molar volumes from the crystal-structure refinements (Stewart and Rooksby 1953; Hawthorne and Ferguson 1975; Yang et al. 1993) and $V_{\beta,1284}$ (see above) with a correction for the volume change of the α-β transition. The resulting parameters for Equations 2 and 3 are: V_{298} = 7.080 ± 0.012 J/(mol·bar), a_1 = (1.39 ± 0.20)·10^{-4} K^{-1}, a_2 = (–2.15 ± 0.51)·10^{-7} K^{-2}, and a_3 = (2.68 ± 0.34)·10^{-10} K^{-3}. This formulation describes the thermal behavior of α- and β-cryolite from ambient to melting temperature at 1 atm; the calculated $V_{\beta,1284}$ = 8.486 J/(mol·bar) reproduces the experimental results (8.49 ± 0.17); see Figure 4. The thermal expansion coefficients at room and transition temperatures vary as follows: α_{298} = 1.39·10^{-4}, α_{832} = 1.33·10^{-4}, and α_{1284} = 4.21·10^{-4} K^{-1}. This increase in the high-temperature region is characteristic for alkali halides (Enck and Dommel 1965; Pathak et al. 1973).

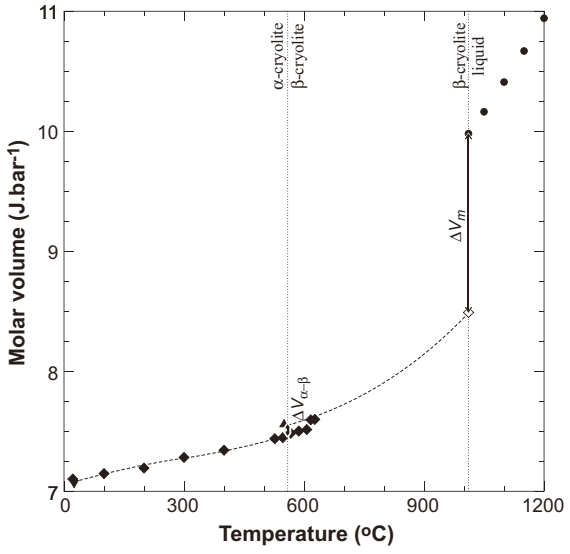

FIGURE 4. Volumetric properties of cryolite and Na_3AlF_6 liquid at 1 atm. Symbols: inverted triangle = cryolite (Hawthorne and Ferguson 1975), upright triangle = cryolite (Stewart and Rooksby 1953), solid diamonds = cryolite (Yang et al. 1993), open diamond = cryolite (this study), circles = liquid (Fernandez and Østvold 1989), dashed curves = volumetric expansion fit (Eq. 2).

DISCUSSION

This section is concerned with three topics: (1) self-dissociation in the cryolite liquid and its effects on enthalpic and volumetric characteristics of melting, (2) similarities in thermal-expansion and melting mechanisms between cryolite and other alkali halides, and (3) significance of solid-solution effects in the "premelting" behavior of cryolite.

The octahedral Al-F coordination in solid cryolite is destabilized during melting and the Na_3AlF_6 liquid exhibits partial self-dissociation into polyhedral aluminofluoride anions $[AlF_n]^{3-n}$ (n = 3–6) and free fluoride anions, F^-, sharing sodium cations, Na^+ (Grjotheim et al. 1959; Frank and Foster 1960; Feng and Kvande 1986; Zhang et al. 2002). The stepwise dissociation is described in species notation as follows:

$$Na_3[AlF_6] = Na_2[AlF_5] + NaF, \quad (4)$$

$$Na_2[AlF_5] = Na[AlF_4] + NaF, \quad (5)$$

and

$$Na[AlF_4] = AlF_3 + NaF, \quad (6)$$

with the following abundances in the cryolite liquid: $Na_3[AlF_6]$ > NaF > $Na[AlF_4]$ > $Na_2[AlF_5]$ >> AlF_3 (e.g., Feng and Kvande 1986; Xu et al. 2001). These speciation mechanisms were independently confirmed by phase equilibria and activity-composition relationships in the NaF-AlF_3 system (Grjotheim 1956; Frank and Foster 1960; Rolin 1961; Sterten and Mæland 1985; Xu et al. 2001) and in situ Raman and nuclear magnetic resonance studies (Solomons et al. 1968; Gilbert et al. 1975; Stebbins et al. 1992; Akdeniz et al. 1998). Enthalpies of these dissociation equilibria are included in the overall enthalpy of melting and are responsible for its higher value, 110 kJ/mol, relative to the end-members: NaF, 33.3 kJ/mol, AlF_3, 112 kJ/mol (Saboungi et al. 1980; Chase 1998). Our aim is to evaluate heat and volumetric portions of melting sensu stricto (i.e., without dissociation) and compare their effects on the $(dT/dp)_m$ slope (Eq. 1).

Estimates of the enthalpy of melting sensu stricto of cryolite to the hypothetical undissociated liquid vary between 73.0 and 97.5 kJ/mol (Grjotheim 1956; Frank 1961; Feng and Kvande 1986; Paučírová et al. 1972; Xu et al. 2001). The lower values come from conductivity measurements and solution modeling (Frank 1961; Xu et al. 2001), whereas the higher values are consistent with phase equilibria and speciation mechanisms in the NaF-AlF_3 system (Grjotheim 1956; Paučírová et al. 1972; Feng and Kvande 1986). The latter were chosen for their mutual consistency and their average was adopted for the hypothetical enthalpy of melting (to undissociated liquid), ΔH_{mc} = 91.6 ± 6.1 kJ/mol. This implies that melting without dissociation accounts for 83.3 ± 6.7% of the total melting enthalpy. The molar volume of the undissociated Na_3AlF_6 component is 9.509 ± 0.057 J/bar (Frank and Foster 1961; Paučírová et al. 1970; Feng and Kvande 1986) and it contributes 68 ± 15% to the total volume change during melting, as measured in this study. This broad similarity (83.3 ± 6.7 vs. 68 ± 15%) indicates that $\Delta H_{mc}/\Delta V_{mc} \sim \Delta H_m/\Delta V_m$, hence the degree of melt dissociation does not have a significant effect on the dp/dT slope of the cryolite melting curve.

Cryolite is one of the intermediate aluminofluoride phases in the NaF-AlF_3 binary system and comparison of its thermal and melting behavior to that of villiaumite, NaF, and to other halides reveals interesting similarities and identifies several "corresponding states". The dT/dp slope of cryolite melting (17.4 ± 1.2 °C/kbar) is identical to that of villiaumite (15.1–18.0 °C/kbar; Clark 1959, Pistorius 1966). The reduced quantities allow additional comparisons with chlorides; the relative volumetric thermal expansion from room conditions to the melting temperature varies as follows: NaCl 13.8% (Deng and Yan 2002), NaF 13.0% (Yagi 1978) vs. Na_3AlF_6 19.6% (this study; including 1.3% due to the α-β transition). The volume change of melting normalized to the volume of the solid phase at the melting temperature, $\Delta V_m/V_{s,Tm}$, is: NaCl 0.246 (Schinke and Sauerweld 1956), NaF 0.246 (Landon and Ubbelohde 1956) vs. Na_3AlF_6 0.176 ± 0.015 (this study). These observations on the thermal and melting behavior of halides suggest that the F-F and Cl-Cl thermal stretching is proportional in sodium halides, but smaller than in aluminofluorides.

The significance of "premelting" vs. solid-solution effects in cryolite melting has remained controversial. Generally, premelting is an endothermic effect occurring as low as 100–200 °C below the equilibrium melting temperature and accounts for 10–20% of the enthalpy of melting (e.g., Ubbelohde 1978). It has been observed in numerous salts and silicates (Ubbelohde 1978; Richet and Fiquet 1991; Richet et al. 1994; George et al. 1998). For cryolite, Landon and Ubbelohde (1957) described an endothermic effect (~0.8 kJ) at 880 °C associated with a rapid increase in the electrical conductivity and attributed it to "premelting" and randomization of the cryolite crystal structure. This phenomenon has not been observed in our experiments but we note that its temperature corresponds to that of the cryolite-villiaumite eutectic (882–885 °C; Phillips et al. 1955; Bukhalova and Mal'tsev 1965). Cryolite forms a minor solid solution within the NaF-AlF_3 system and its range expands with increasing temperature from $Na_{3.000–2.993}Al_{1.000–1.002}F_6$ at 560 °C through $Na_{2.985–2.929}Al_{1.005–1.024}F_6$ at 880 °C to a maximum on the liquidus curve at $Na_{2.924}Al_{1.025}F_6$ (Dewing 1978, 1997). The cryolite solid solution boundary systematically shifts toward higher Al/Na ratios in favor of the two-phase cryolite + villiaumite field with increasing temperature, thus Na-rich cryolite solid-solutions undergo a small amount of villiaumite exsolution below ~882 °C and minor partial melting above ~885 °C. The "premelting" effect seen in some previous studies (Landon and Ubbelohde 1957) is most probably related to incipient eutectic melting of villiaumite exsolutions (or impurities). The composition of our starting material, $Na_{2.93(4)}Al_{1.00(3)}F_6$, is in excellent agreement with the solid-solution range at high temperature and explains the absence of "premelting" or villiaumite melting in our study.

This minor compositional variation in cryolite is difficult to detect by microbeam or wet-chemical techniques; if measurable it can provide information on temperature of cryolite crystallization in natural conditions. The Na_3Al_{-1} exchange differs from the more extensive Na_2Ca_{-1} substitution (Craig and Brown 1980; Chartrand and Pelton 2002), which can easily be verified by calcium analysis.

Geological implications

We have measured the pressure dependence of the α-β transition and melting temperatures of cryolite up to 100 MPa and derived the associated volumetric and thermal-expansion properties. Cryolite is the most common aluminofluoride mineral (Bailey 1980) and it becomes a fluorine-buffering phase in peralkaline silicic magmas and their metasomatic products (Kovalenko et al. 1995; Pauly and Bailey 1999; Goodenough et al. 2000; Dolejš and Baker 2004a). Due to the strong short-range ordering in fluorine-bearing aluminosilicate melts and the formation of aluminofluoride complexes (Manning et al. 1980; Schaller et al. 1992; Zeng and Stebbins 2000), cryolite is a preferred component for thermodynamic models of peralkaline granitic and rhyolitic systems (cf. Burnham 1997). The present results complement thermochemical data by Chase (1998) and Dolejš and Baker (2004a) and allow for thermodynamic modeling using Na_3AlF_6 (s,l) at elevated temperatures and pressures.

During magmatic differentiation, cryolite has low solubility and saturates early in peralkaline fluorine-bearing melts (Dolejš and Baker 2001). Its crystallization moderates fluorine enrichment in the residual melt, but in the presence of other alkali halides, immiscible salt melts or brines may form due to the strong solidus depressions in the chloride-fluoride systems. Cryolite is compatible with NaF and NaCl, whereas elpasolite, Na_2KAlF_6 (Frondel 1948) is, in addition, compatible with potassium halides KF and KCl (Sorrell and Groetsch 1986), with the following eutectic temperatures (at 1 atm): cryolite-elpasolite at 913 °C, cryolite-villiaumite at 882–885 °C, villiaumite-halite at 678–680 °C, cryolite-villiaumite-halite at 674 °C, and villaumite-halite-sylvite at 590–606 °C (Fedotieff and Iljinsky 1913; Sauerwald and Dombois 1954; Phillips et al. 1955; Kuvakin and Kusakin 1959; Bukhalova and Mal'tsev 1965). In the presence of H_2O, these halide melts (brines) will evolve toward aqueous fluids either continuously or by boiling (Bodnar et al. 1985; Hovey et al. 1990; Urusova and Ravich 1966; Kotelnikova and Kotelnikov 2002; cf. Macdonald et al. 1973). Our finding that the pressure dependence of the cryolite melting temperature is very similar to that of other halide end-members (NaF, KF, NaCl, and KCl; Clark 1959; Pistorius 1966) suggests consistent changes in phase-diagram topologies with increasing pressure and lends support to their application to understanding the behavior of multicomponent fluoride-chloride brines in the hydrothermal aureoles of peralkaline intrusions.

Acknowledgments

This study is a portion of the senior author's Ph.D. thesis at McGill University, supported by the J.B. Lynch and Carl Reinhardt fellowships. Research funding was provided by the Geological Society of America and the Society of Economic Geologists student grants to D.D. and by the Natural Sciences and Engineering Research Council to D.R.B. We are grateful to H. Keppler, R. Linnen, P. Ihinger, and T. Grove for sharing information on the TZM pressure-vessel design. R.F. Martin provided us with the reference to the original description of cryolite.

References cited

Abildgaard, P.C. (1799) Norwegische Titanerze und andre neue Fossilien. Scherer's Allgemeines Journal der Chemie, 2, 502.

Akdeniz, Z., Cicek, Z., Pastore, G., and Tosi, M.P. (1998) Ionic clusters in aluminum-sodium fluoride melts. Modern Physics Letters B, 12, 995–1002.

Bailey, J.C. (1980) Formation of cryolite and other aluminofluorides: a petrological review. Bulletin of the Geological Society Denmark, 29, 1–45.

Bodnar, R.J., Burnham, C.W., and Sterner, S.M. (1985) Synthetic fluid inclusions in natural quartz. III. Determination of phase equilibrium properties in the system H_2O-NaCl to 1000°C and 1500 bars. Geochimica et Cosmochimica Acta, 49, 1861–1873.

Brosset, C. (1937) Preparation and crystal structure of the compounds $TlAlF_4$ and Tl_2AlF_5. Zeitschrift für anorganische und allgemeine Chemie, 235, 139–147.

Bukhalova, G.A. and Mal'tsev, V.T. (1965) The K, Na ‖ AlF_6, F system. Russian Journal of Inorganic Chemistry, 10, 100–102.

Burnham, C.W. (1997) Magmas and hydrothermal fluids. In H.L. Barnes, Ed., Geochemistry of Hydrothermal Ore Deposits, 3rd ed., p. 63–123. Wiley, New York.

Chartrand, P. and Pelton, A.D. (2002) A predictive thermodynamic model for the Al-NaF-AlF_3-CaF_2-Al_2O_3 system. Light Metals, 2002, 245–252.

Chase, M.W., Ed. (1998) NIST-JANAF thermochemical tables. Journal of Physical and Chemical Reference Data, Monograph, 9, 1951 p.

Clark, S.P., Jr. (1959) Effect of pressure on the melting point of eight alkali halides. Journal of Chemical Physics, 31, 1526–1531.

Craig, D.F. and Brown, J.J., Jr. (1980) Phase equilibria in the system CaF_2-AlF_3-Na_3AlF_6 and part of the system CaF_2-AlF_3-Na_3AlF_6-Al_2O_3. Journal of the American Ceramic Society, 63, 254–261.

Dawson, R., Brackett, E.B., and Bracket, T.E. (1963) A high temperature calorimeter; the enthalpies of α-aluminum oxide and sodium chloride. Journal of Physical Chemistry, 67, 1669–1671.

Denbigh, K.G. (1981) The principles of chemical equilibrium: with applications in chemistry and chemical engineering, 494 p. Cambridge University Press, U.K.

Deng, X.-Q. and Yan, Z.-T. (2002) Analysis of *P-V-T* relationships and thermodynamic properties for some alkali halides. Journal of Physics and Chemistry of Solids, 63, 1737–1744.

Dewing, E.W. (1978) Thermodynamics of the system NaF-AlF_3: Part V. Solid solution in cryolite. Metallurgical Transactions, 9B, 687–690.

——— (1997) Thermodynamics of the system NaF-AlF_3: Part VII. Non-stoichiometric solid cryolite. Metallurgical and Materials Transactions, 28B, 1095–1097.

Dolejš, D. and Baker, D.R. (2001) Chemical properties of evolved granitic magmas: the role of fluorine. Geological Society of America Abstracts, 33, A333.

——— (2002) Melting equilibria of F-bearing silicic magmas: an experimental study. Geochimica et Cosmochimica Acta, 66, A-190.

——— (2004a) Thermodynamic analysis of the system Na_2O-K_2O-CaO-Al_2O_3-SiO_2-H_2O-F_2O_{-1}: Stability of fluorine-bearing minerals in felsic igneous suites. Contributions to Mineralogy and Petrology, 146, 762–778.

——— (2004b) Thermodynamic model of the Na-Al-Si-O-F melts. Eos Transactions of the American Geophysical Union, 85 (Supplement), V51C-03.

Edwards, J.D., Taylor, C.S., Cosgrove, L.A., and Russell, A.S. (1953) Electrical conductivity and density of molten cryolite with additives. Journal of the Electrochemical Society, 100, 508–512.

Enck, F.D. and Dommel, J.G. (1965) Behavior of the thermal expansion of NaCl at elevated temperatures. Journal of Applied Physics, 36, 839–844.

Fedotieff, P.P. and Iljinsky, W. (1913) Beiträge zur Elektrometallurgie des Aluminiums. Zeitschrift für anorganische Chemie, 80, 113–154.

Feng, X.N. and Kvande, H. (1986) Dissociation equilibria in molten cryolite: The presence of AlF_5^{2-} ions. Acta Chemica Scandinavica, A40, 622–630.

Fernandez, R. and Østvold, T. (1989) Surface tension and density of molten fluorides and fluoride mixtures containing cryolite. Acta Chemica Scandinavica, A43, 151–159.

Frank, W.B. (1961) Thermodynamic considerations in the aluminum-producing electrolyte. Journal of Physical Chemistry, 65, 2081–2087.

Frank, W.B. and Foster, L.M. (1960) The constitution of cryolite and NaF-AlF_3 melts. Journal of Physical Chemistry, 64, 95–98.

Frondel, C. (1948) New data on elpasolite and hagemannite. American Mineralogist, 32, 84–87.

George, A.M., Richet, P., and Stebbins, J.F. (1998) Cation dynamics and premelting in lithium metasilicate (Li_2SiO_3) and sodium metasilicate (Na_2SiO_3): A high-temperature NMR study. American Mineralogist, 83, 1277–1284.

Gilbert, B., Mamantov, G., and Begun, G.M. (1975) Raman spectra of aluminum fluoride containing melts and the ionic equilibrium in molten cryolite type mixtures. Journal of Chemical Physics, 62, 950–955.

Goodenough, K.M., Upton, B.G.J., and Ellam, R.M. (2000) Geochemical evolution of the Ivigtut granite, South Greenland: a fluorine-rich "A-type" intrusion. Lithos, 51, 205–221.

Grjotheim, K. (1956) Contribution to the theory of aluminum electrolysis. Konunglegur Norske Vitenskaper Selskabs Skrifter, 2, 1–90.

Grjotheim, K., Halvorsen, T., and Urnes, S. (1959) The phase diagram of the system Na_3AlF_6-Na_2SO_4 and the dissociation of the cryolite anion in molten sodium sulphate. Canadian Journal of Chemistry, 37, 1170–1175.

Grjotheim, K., Krohn, C., Malinovský, M., Matiášovský, M., and Thonstadt, J., Eds. (1977) Aluminum electrolysis: The chemistry of the Hall-Heroult process, 350 p. Aluminium-Verlag, Düsseldorf.

Hawthorne, F.C. (1984) The crystal structure of stenonite and the classification of the aluminofluoride minerals. Canadian Mineralogist, 22, 245–251.

Hawthorne, F.C. and Ferguson, R.B. (1975) Refinement of the crystal structure of cryolite. Canadian Mineralogist, 13, 377–382.

Hovey, J.K., Pitzer, K.S., Tanger, J.C. IV, Bischoff, J.L., and Rosenbauer, R.J. (1990) Vapor-liquid phase equilibria of KCl-H_2O mixtures: equation-of-state representation for KCl-H_2O and NaCl-H_2O. Journal of Physical Chemistry, 94, 1175–1179.

Kleppa, O J. and Julsrud, S. (1980) Thermodynamics of charge-unsymmetrical anion mixtures. I. The liquid systems AF-A_2SO_4. Acta Chemica Scandinavica, A34, 655–665.

Kogarko, L.N. (1967) Lamination area in melts of the system Si, Al, Na ‖ O, F. Doklady Akademii Nauk SSSR, 176, 203–205.

Kogarko, L.N. and Krigman, L.D. (1975) Immiscibility in fluorosilicate systems. Physics and Chemistry of Glasses, 1, 61–65.

Kojima, H., Whiteway, S.G., and Masson, C.R. (1968) Melting points of inorganic fluorides. Canadian Journal of Chemistry, 46, 2968–2971.

Koster van Groos, A.F. (1979) Differential thermal analysis of the system NaF-Na_2CO_3 to 10 kbar. Journal of Physical Chemistry, 83, 2976–2978.

Kotelnikova, Z.A. and Kotelnikov, A.R. (2002) Synthetic NaF-bearing fluid inclusions. Geochemistry Intnernational, 40, 594–600.

Kovalenko, V.I., Tsaryeva, G.M., Goreglyad, A.V., Yarmolyuk, V.V., Troitsky, V.A., Hervig, R.L., and Farmer, G.L. (1995) The peralkaline granite-related Khaldzan-Buregtey rare metal (Zr, Nb, REE) deposit, western Mongolia. Economic Geology, 90, 530–547.

Kuvakin, M.A. and Kusakin, P.S. (1959) The sodium fluoride-aluminium fluoride-sodium chloride system. Russian Journal of Inorganic Chemistry, 4, 1188–1190.

Landon, G.J. and Ubbelohde, A.R. (1956) Volume changes on melting ionic crystals. Transactions of the Faraday Society, 52, 647–651.

——— (1957) Melting and crystal structure of cryolite (3NaF, AlF_3). Proceedings of the Royal Society (London), 240A, 160–172.

Lin, P.L., Pelton, A.D., and Saboungi, M.-L. (1982) Computer analysis pf phase diagrams and thermodynamic properties of cryolite based systems: Part II. The AlF_3-CaF_2-LiF, AlF_3-CaF_2-NaF, and CaF_2-LiF-NaF systems. Metallurgical Transactions, 13B, 61–69.

Macdonald, R., Upton, B.G.J., and Thomas, J.E. (1973) Potassium- and fluorine-rich hydrous phase coexisting with peralkaline granite in south Greenland. Earth and Planetary Science Letters, 18, 271–222.

Majumdar, A.J. and Roy, R. (1965) Test of the applicability of the Clapeyron relation of a few cases of solid-solid transitions. Journal of Inorganic and Nuclear Chemistry, 27, 1961–1973.

Malinovský, M. (1984) Cryometric determination of the enthalpy of fusion of sodium cryolite. Chemicke Zvesti, 38, 165–172.

Manning, D.A.C., Hamilton, D.L., Henderson, C.M.B., and Dempsey, M.J. (1980) The probable occurrence of interstitial Al in hydrous, F-bearing and F-free aluminosilicate melts. Contributions to Mineralogy and Petrology, 75, 257–262.

O'Brien, C.J. and Kelley, K.K. (1957) High-temperature heat contents of cryolite, anhydrous aluminum fluoride, and sodium fluoride. Journal of the American Chemical Society, 79, 5616–5618.

Pabst, A. (1950) A structural classification of fluoroaluminates. American Mineralogist, 35, 149–165.

Pathak, P.D., Trivedi, J.M., and Vasavada, N.G. (1973) Thermal expansion of NaF, KBr and RbBr and temperature variation of the frequency spectrum of NaF. Acta Crystallographica, A29, 477–479.

Paučírová, M., Matiašovský, K., and Malinovský, M. (1970) Contribution to the study of the structure of molten LiF-AlF_3 and NaF-AlF_3 mixtures. Revue Roumaine de Chimie, 15, 201–208.

——— (1972) Structure and the thermodynamic properties of molten compounds of the type M_3AlF_6. II. Thermodynamic properties. Revue Roumaine de Chimie, 17, 809–817.

Pauly, H. and Bailey, J.C. (1999) Genesis and evolution of the Ivigtut cryolite deposit, SW Greenland. Meddelelser om Grønland, Geoscience, 37, 60 p.

Phillips, N.W.F., Singleton, R.H., and Hollingshead, E.A. (1955) Liquidus curves for aluminum cell electrolyte. II. Ternary systems of cryolite-alumina with sodium fluoride, sodium chloride, and aluminum fluoride. Journal of the Electrochemical Society, 102, 688–690.

Pistorius, C.W.F.T. (1966) Effect of pressure on the melting points of the sodium halides. Journal of Chemical Physics, 45, 3513–3519.

Prigogine, I. and Defay, R. (1954) Chemical Thermodynamics, p. 543. Longmans, London.

Reed, B.C. (1989) Linear least-squares fits with errors in both coordinates. American Journal of Physics, 57, 642–646 (erratum: 58, 189).

——— (1992) Linear least-squares fits with errors in both coordinates. II: Comments on parameter variances. American Journal of Physics, 60, 59–62.

Richet, P. and Fiquet, G. (1991) High-temperature heat capacity and premelting of minerals in the system MgO-CaO-Al_2O_3-SiO_2. Journal of Geophysical Research, 96, 445–456.

Richet, P., Ingrin, J., Mysen, B.O., Courtial, P., and Guillet, P. (1994) Premelting

effects in minerals; an experimental study. Earth and Planetary Science Letters, 121, 589–600.
Rolin, M. (1961) Sur la structure ionique de la cryolithe pure fondue. IV. Compatibilité du schéma. $AlF_6^{3-} = AlF_4^- + 2\ F^-$ avec le diagramme expérimental. Bulletin de la Societé Chimique de France, 1960, 681–685.
Rutlin, J.L. (1998) Chemical reactions and mineral formation during sodium aliminium fluoride attack on aluminosilicate and anorthite based refractories, 167 p. Dr-Ing. thesis, NTNU Trondheim, Norway.
Sabougi, M.L., Lin, P.L., Cerisier, P., and Pelton, A.D. (1980) Computer analysis of phase diagrams and thermodynamic properties of cryolite based system: I. The AlF_3-LiF-NaF system. Metallurgical Transactions, 11B, 493–501.
Sauerwald, F. and Dombois, H.E. (1954) Über die allgemeinen Formen der Dreistoff-Diagramme mit zwei eutektischen binären Systemen und einem binären Mischkristallsystem mit Mischungslücke und kritischem Punkt, sowie das System KCl-NaCl-NaF. Zeitschrift für anorganische und allgemeine Chemie, 277, 60–72.
Schaller, T., Dingwell, D.B., Keppler, H., Knoeller, W., Merwin, L., and Sebald, A. (1992) Fluorine in silicate glasses: a multinuclear nuclear magnetic resonance study. Geochimica et Cosmochimica Acta, 56, 701–707.
Schinke, H. and Sauerwald, F. (1956) Density measurements. XVIII. Changes of volume during melting and the melting process in salts. Zeitschrift für anorganische und allgemeine Chemie, 287, 313–324.
Solomons, C., Clarke, J.H.R., and Bockris, J. O'M. (1968) Identification of the complex ions in liquid cryolite. Journal of Chemical Physics, 49, 446–459.
Sorrell, C.A. and Groetsch, J.G., Jr. (1986) Subsolidus compatibility in the system NaCl-KCl-$AlCl_3$-NaF-KF-AlF_3. Journal of the American Ceramic Society, 69, 333–338.
Spearing, D.R., Stebbins, J.F., and Farnan, I. (1994) Diffusion and the dynamics of displacive phase transitions in cryolite (Na_3AlF_6) and chiolite ($Na_5Al_3F_{14}$): Multi-nuclear NMR studies. Physics and Chemistry of Minerals, 21, 373–386.
Stebbins, J.F., Farnan, I., Dando, N., and Tzeng, S.-Y. (1992) Solids and liquids in the NaF-AlF_3-Al_2O_3 system: A high-temperature NMR study. Journal of the American Ceramic Society, 75, 3001–3006.
Sterten, A. and Mæland, I. (1985) Thermodynamics of molten mixtures of Na_3AlF_6-Al_2O_3 and NaF-AlF_3. Acta Chemica Scandinavica, A39, 241–257.
Stewart, E.G. and Rooksby, H.P. (1953) Transitions in crystal structure of cryolite and related fluorides. Acta Crystallographica, 6, 49–52.
Stølen, S. and Grande, T. (2004) Chemical thermodynamics of materials: Macroscopic and microscopic aspects, 395 p. Wiley, Chichester.
Strunz, H. and Nickel, E.H. (2001) Strunz mineralogical tables. Chemical-structural mineral classification system, 870 p. Schweizerbart, Stuttgart.
Ubbelohde, A.R. (1978) The molten state of matter, 454 p. Wiley, New York.
Urusova, M.A. and Ravich, M.I. (1966) Phase equilibria in the potassium fluoride-water system at elevated temperatures. Russian Journal of Inorganic Chemistry, 11, 353–357.
Wyllie, P.J. and Raynor, E.J. (1965) DTA (differential thermal analysis) and quenching methods in the system CaO-CO_2-H_2O. American Mineralogist, 50, 2077–2082.
Xu, Q., Ma, Y., and Qiu, Z. (2001) Calculation of thermodynamic properties of LiF-AlF_3, NaF-AlF_3 and KF-AlF_3. Calphad, 25, 31–42.
Yagi, T. (1978) Experimental determination of thermal expansivity of several alkali halides. Journal of Physics and Chemistry of Solids, 39, 563–571.
Yamada, M., Tago, M., Fukusako, S., and Horibe, A. (1993) Melting point and supercooling characteristics of molten salt. Thermochimica Acta, 218, 401–411.
Yang, H., Ghose, S., and Hatch, D.M. (1993) Ferroelastic phase transition in cryolite, Na_3AlF_6, a mixed fluoride perovskite: High temperature single crystal X-ray diffraction study and symmetry analysis of the transition mechanism. Physics and Chemistry of Minerals, 19, 528–544.
Zeng, Q. and Stebbins, J.F. (2000) Fluoride sites in aluminosilicate glasses: High-resolution ^{19}F NMR results. American Mineralogist, 85, 863–867.
Zhang, Y., Gupta, S., Sahai, Y., and Rapp, R.A. (2002) Modeling of the solubility of alumina in the NaF-AlF_3 system at 1300 K. Metallurgical and Materials Transactions, 33B, 315–319.

MANUSCRIPT RECEIVED JULY 20, 2004
MANUSCRIPT ACCEPTED APRIL 20, 2005
MANUSCRIPT HANDLED BY LEE GROAT